Radio-Relay Antenna Pointing for Controlled Interference with Geostationary Satellites

By C. W. LUNDGREN and A. S. MAY

(Manuscript received July 23, 1969)

We present analytical methods (i) *for calculating microwave radio refraction for negative and positive initial ray angles accounting for station height and* (ii) *for determining refraction-corrected ranges of antenna pointing azimuth within which mutual interference with geostationary satellites in shared frequency bands is likely.*

I. INTRODUCTION

When radio-relay and communication satellite systems share frequency bands, as they do at 4 and 6 GHz, it is necessary to impose restrictions on both systems so that interference is not excessive. The CCIR (International Radio Consultative Committee) recommends that radio-relay antennas maintain a specified angular separation with respect to the geostationary (stationary equatorial) orbit or, where this is not practicable, the application of power limitations to terrestrial radio transmitters involving reception at the satellite. While the above restrictions protect satellites, designers of terrestrial systems should be aware of possible interference into radio-relay systems from satellite radiation arriving at low elevation angles and close to the on-beam directions of receiving antennas. Because the dielectric constant of the earth's atmosphere varies with altitude, the radio-relay beam is not straight, and atmospheric refraction must be considered when computing the directions of radio beams for which the restrictions apply.

1.1 *Simplified Exposure Model*

Figure 1 introduces the geometry of the problem and illustrates significant trends and limits. Radio-relay site P located at North Latitude φ degrees is shown as viewed from above the earth. An arc of the geostationary satellite orbit is also shown. The orbit longitude of point

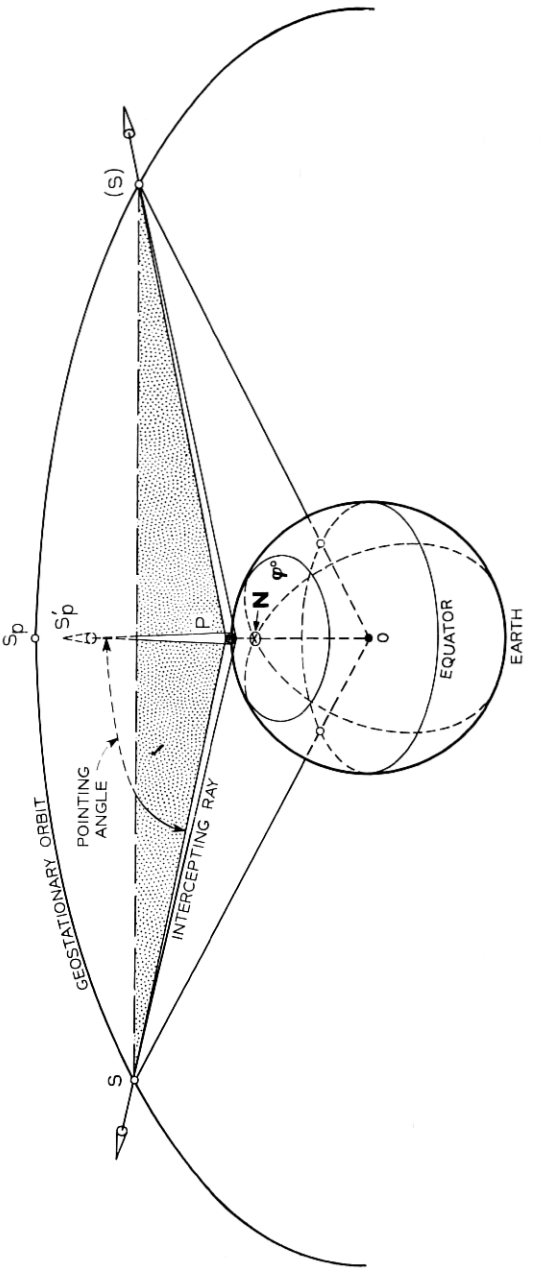

Fig. 1 — Geometry relating unrefracted horizontal radio-relay beams and the geostationary orbit.

S_p and the earth longitude of site P coincide numerically (that is, S_p is in the direction of true south, $\mathbf{PS}'_p$, observed from P).

Two radio rays from P intercept the orbit symmetrically at points S. The controlling geometric relationships are based upon triangles formed by points S, P, and geocenter O. Angle O–P–S is determined by the elevation angle of the radio-relay antenna including ray bending due to atmospheric refraction. A special case is depicted in Fig. 1, wherein unbent intercepting rays **PS** and also ray $\mathbf{PS}'_p$ are assumed to lie in the local horizontal plane at P and remain tangent to the earth sphere at P. Thus, angles S–P–S'_p are always antenna pointing angles to orbit interception referred to "true south."

It is instructive to visualize the relationship between latitude φ at P and the location of orbit intercepts S, for a given fixed triangle OPS. As points S approach S_p, the constraints imposed above require that the station latitude φ approach a maximum latitude "visible" to the orbit. The resulting single pointing direction to orbit intercept is due south (from P to S_p). Conversely, the maximum separation between points S and S_p obtains when φ is zero (for site P located on the equator). Since both intercepting rays are tangent to the equator at P, the limiting pointing directions are due west and due east.

Note that a rotation in azimuth of the antenna (about the local vertical axis at P) between known orbit-intercept directions results in radio rays **PS** which fall below the orbit as viewed from P; rotations beyond these "critical azimuths" result in rays above the orbit.

1.2 *Computations*

Given the latitude and elevation angle of a microwave radio-relay antenna, one can calculate the pointing azimuth for which, neglecting refraction, the main beam axis intercepts the geostationary orbit. This calculation is repeated to produce screening charts like Fig. 2. Such charts are adequate for quickly determining a hazard condition, but often the true critical azimuths must be approached closely while maintaining tolerable interference levels.

A graphical procedure proposed for the convenience of system planners provides pointing angle estimates for most stations when caution is exercised in those steps accounting for atmospheric refraction.[1] An analytical technique adaptable to machine calculation is also required for rapid, accurate screening of large numbers of existing and proposed radio-relay sites for potential interference exposures. Precise evaluations are required for cases of unavoidable exposure.

The method described in following sections can be used by the system

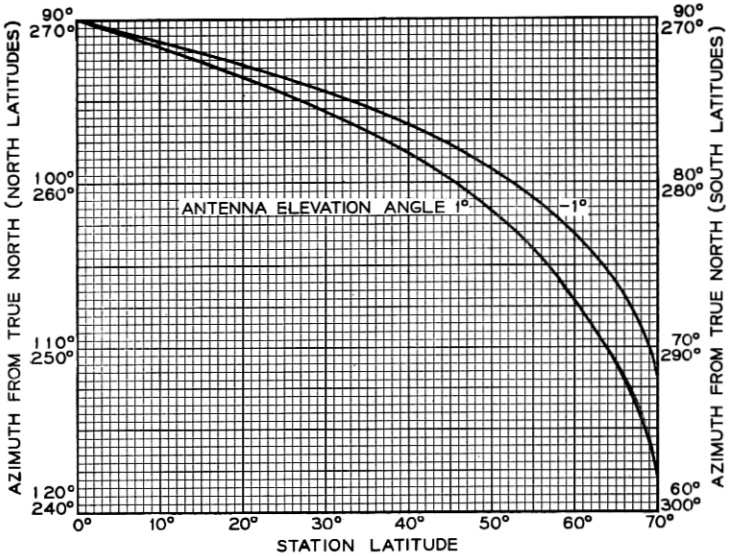

Fig. 2 — Screening chart, neglecting refraction.

planner to determine critical azimuths and the ranges of azimuths to be avoided (accounting for atmospheric refraction) for prescribed minimum angular separations between main beam axes and the geostationary orbit.

The Central Radio Propagation Laboratory (CRPL) Exponential Reference Atmosphere is adopted for the generation of microwave radio refraction curves by accounting for station heights and negative antenna elevation angles, for several representative refractive indexes.[2] Earlier extrapolations are based upon upper limits of the total bending associated with assumed earth-grazing rays.[3,4]

A refraction anomaly arising from a temperature inversion, storm, ducting, or other departure from an assumed representative radial ray-bending model precludes an absolutely confident evaluation of any given exposure at a given time. These phenomena are usually localized. However, the intent of these computations is to protect the geostationary orbit against continuous interference arising simultaneously from a large number of terrestrial systems.

Following a development of the refraction model, we derive the critical pointing azimuth corresponding to orbit intercept. The geocentered longitude displacement between the radio-relay site and the point where the refracted beam intercepts the orbit is next determined by spherical

geometry. Then the apparent slope* of the geometric orbit trace, as if viewed unbent by refraction from the station, is obtained corrected for aspect (also dependent upon antenna elevation angle and concomitant refraction). Using the refraction data converted to geometric elevation angles (as without ray bending or obstruction), the geometric orbit is adjusted to the apparent position and shape that would be observed at the radio site. This apparent orbit is hereafter termed the refracted orbit. Subsequent sections describe the determination of azimuth zones to be avoided for prescribed beam—orbit separations and the permissible transmitted power. Appendices are included to: provide means for estimating initial ray angles from commonly available radio-relay information when actual antenna angles are unknown; solve by manual calculation a representative numerical example, giving the applicable equations for each step; and verify governing equations using a different analytical approach.

II. DETERMINATION OF REFRACTION FOR POSITIVE AND NEGATIVE ANTENNA ELEVATION ANGLES

2.1 *Ray Tracing Equations*

In the following equations θ_o is the initial angle† of a ray as it leaves the earth's surface and τ is the total refractive bending corresponding to θ_o. Figure 3 illustrates this relationship and shows the geometric director with elevation angle ϵ to an intercept with the geostationary orbit at S. Also shown on an arc through S centered at P is the apparent position of the intercept S_a and a horizontal reference, zero-elevation point A. The latter relationships are used in a subsequent section to describe a method for constructing the refracted orbit.

Angle ϵ is approximately, but in general not identical to, $\theta_0 - \tau$‡. However, this approximation is reasonable for rays between terrestrial antennas and geostationary satellites well beyond the earth's atmosphere when relatively small effects of parallax associated with the controlling portion of the atmosphere near the earth's surface are neglected.[5]

Figure 4 depicts a ray entering the earth's atmosphere and the result-

* The first derivative with respect to pointing azimuth (azimuth-elevation plot of the orbit) is more completely defined in Section V.

† θ_o is generally used in ray-tracing equations to denote the initial ray elevation angle with respect to the local horizontal and is synonymous with α_o used in subsequent sections to denote a radio-relay antenna beam elevation angle (namely, α in Figs. 6).

‡ Calculations using equation (5) show that the actual ray angle with respect to the geocenter differs from that resulting from the assumption $\epsilon = \theta_o - \tau$ by approximately 1.5 minutes of arc for limiting conditions used herein.

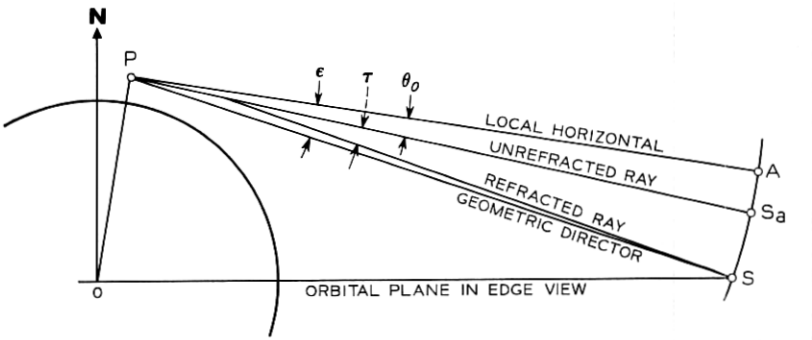

Fig. 3 — Refracted ray.

ing path of the ray due to the refractive gradient. Depending upon the angle of arrival of the ray when it enters the atmosphere, the refraction causes it to intercept the earth, graze the earth, or become tangent to a unique earth-centered sphere at some height above the surface. If the ray does not intercept the earth it continues out into space again, being subjected to approximately the same refraction in exit as it encountered upon entering.

At any point on the ray trace, the angle the ray makes with the local horizontal at that point is denoted by θ. The angle between the tangents to the ray at any two points (a, b) is a measure of the refractive bending between them and is denoted by $\tau(a, b)$.

The following presentation of refraction is based largely upon equations given in Refs. 2, 6, and 7 for zero or positive initial ray angles and as interpreted by the authors for application to negative angles. Appropriate uses of the equations and their application to the problem are

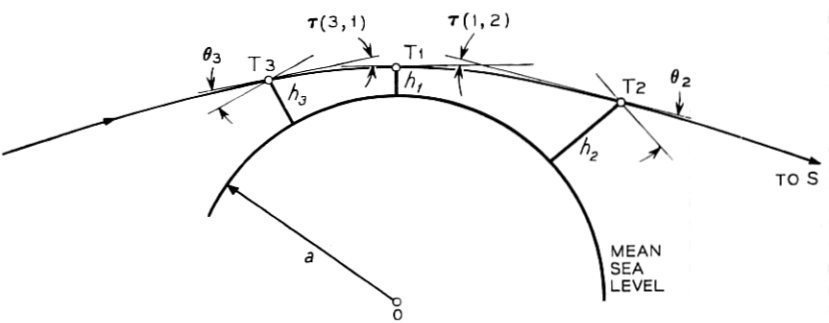

Fig. 4 — Maximally refracted nongrazing ray.

explained, but the reader is directed to the references for complete derivations and limitations including sensitivities to the microwave frequencies involved.

The radio refractive index n varies with atmospheric pressure, relative humidity, saturation vapor pressure and temperature. The lower limit for n is unity—no atmosphere, while the upper limit is determined by local climatic conditions. For the southeastern section of the United States, a typical range of n at mean sea level is 1.00025 to 1.0004. In equations involving refraction it is convenient to express refractivity as N where $N = (n - 1) \times 10^6$ or, for this case, N values are 250 and 400 (N units). The average decay of N is approximately exponential with height and the difference in N between the surface and a height of 1 km above the surface is given by[2]

$$\triangle N = -7.32 \exp (0.005577 N_s). \tag{1}$$

The subscript s denotes N at the surface. The decay constant with height is expressed by[2]

$$C_s = \ln \frac{N_s}{N_s + \triangle N}. \tag{2}$$

N at any height h (kilometers above the radio site surface elevation) is[2]

$$N_h = N_s \exp [-C_s(h - h_s)], \tag{3}$$

where h_s is the surface elevation above mean sea level corresponding to N_s.

N_s is sensitive to local elevations and hence, charts of N_s for mountainous regions are difficult to use because the N_s contours are irregular and closely spaced. Therefore, obtaining an appropriate value of N_s for use in equations (1), (2), and (3) for a particular site is often difficult. However, charts are available giving N_s reduced to mean sea level equivalents N_o which, in effect, reduce the height-dependent N_s values to a common base.[8] Since charts of N_o are more easily interpreted and a single value of N_o usually applies over a large geographical area, they are used in this paper.

N_o and $N_s(h)$ are related[6] by $N_o = N_s \exp (-h/7)$. Conversely, for a given value of N_o, N_s for surface height h_s above mean sea level is determined from the expression

$$N_s = N_o \exp (-h_s/7), \qquad h_s \geqq 0. \tag{4}$$

The N_s value obtained from equation (4) is used in equations (1), (2),

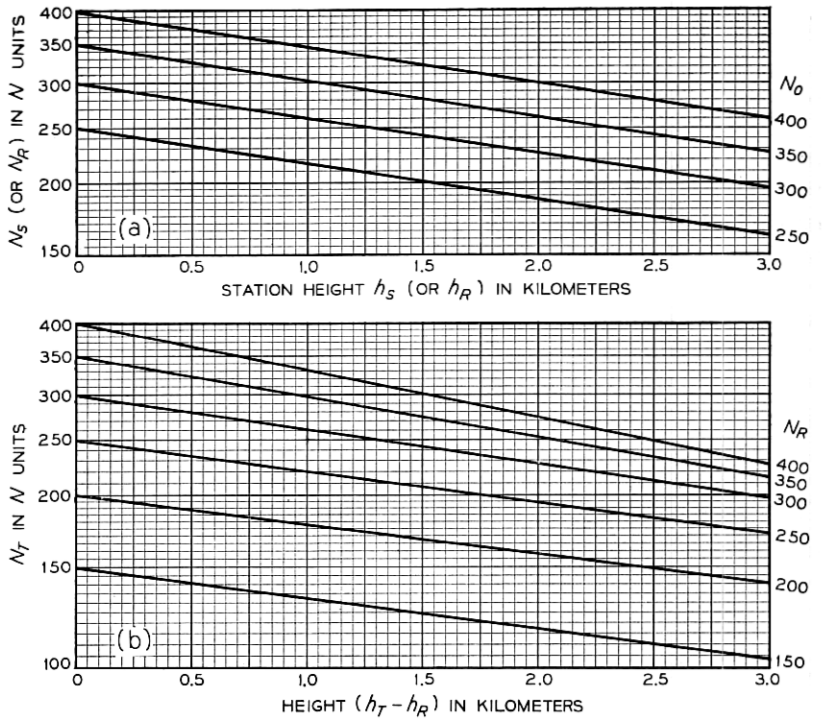

Fig. 5(a) — Radio refractivity conversion — N_o to N_s (or N_R).
Fig. 5(b) — Radio refractivity conversion — N_R to N_T.

and (3). Figure 5a was generated using equation (4) and, for manual calculations, is convenient for determining N_s.

The conversion between N_o and N_s above considers only the dry air effects of temperature and pressure related to the difference in elevation between mean sea level and the station surface height, whereas constants of the expression given for $\triangle N$ account for all terms contributing to a change in refractivity of the atmosphere with elevation above the surface height.

A relationship exists between angle θ_o at the point of origin of the ray and θ at any other point on the ray trace which is expressed by

$$(1 + N_s \times 10^{-6})(a + h_s) \cos \theta_o = (1 + N_h \times 10^{-6})(a + h) \cos \theta = C, \quad (5)$$

where C is a constant and a is the earth's radius at mean sea level (in kilometers). Thus, angle θ for any point on the ray trace is determined.

The incremental bending of the ray between closely spaced points on the trace is given by

$$\tau(1, 2) = -\int_{n_1}^{n_2} \frac{dn}{n} \cot \theta. \tag{6}$$

As suggested by Schulkin, the term $1/n$ is taken as unity with an error of less than 0.0001 in the computed refraction and, for an iterative solution, equation (6) is expressed as[7]

$$\tau(1, 2) = -\int_{\Delta n_1}^{\Delta n_2} \cot \theta \, d\Delta n. \tag{7}$$

Shulkin also shows[7] that equation (7) is approximated by $(\Delta n1 - \Delta n2)/\theta_m$ where Δn is $n - 1$ and θ_m is $(\theta 1 + \theta 2)/2$. Hence the incremental bending between two closely spaced points on the ray trace is expressed by

$$\tau(1, 2) = \frac{2(N_1 - N_2) \times 10^{-6}}{\theta_1 + \theta_2} \text{ rad.}, \quad 0 \leqq \theta_o \leqq 10°, \tag{8}$$

where N_1 and N_2, θ_1 and θ_2 are the N values and ray angles (in radians), respectively, at the closely spaced points.

2.2 *A Method for Calculating Refraction*

The following paragraphs describe a procedure for calculating refraction curves of the form in Figs. 6 for any values of N_o which is also applicable for the direct calculation of refraction corrections.

2.2.1 *Zero and Positive Initial Angles* $(+\theta_o)$

First assume a value of N_o, a station height h_s, and an initial ray angle θ_0. Equation (4) is used to determine N_s for height h_s and equations (1), (2), and (3) to determine N for a height h, where $h = h_s + \Delta h$*. Equations (5) and (8) then give the ray angle θ at the incremental height and the bending τ in the first increment. For each successive increment of height, the previously solved-for values of N and θ become the initial values for equations (3), (5), and (8). The values of τ for each iteration are accumulated to give the total bending for h_s and θ_o. Repeating the above procedure with other values of θ_o results in data points to be used in plotting the refraction curve for the assumed station height h_s. A complete repetition of the above, beginning with

* Incremental heights must be small in the lower atmosphere where n changes rapidly but may increase at the higher elevations. However, for the generation of Fig. 6, a constant increment of 0.25 km was used to a height of 90 km.

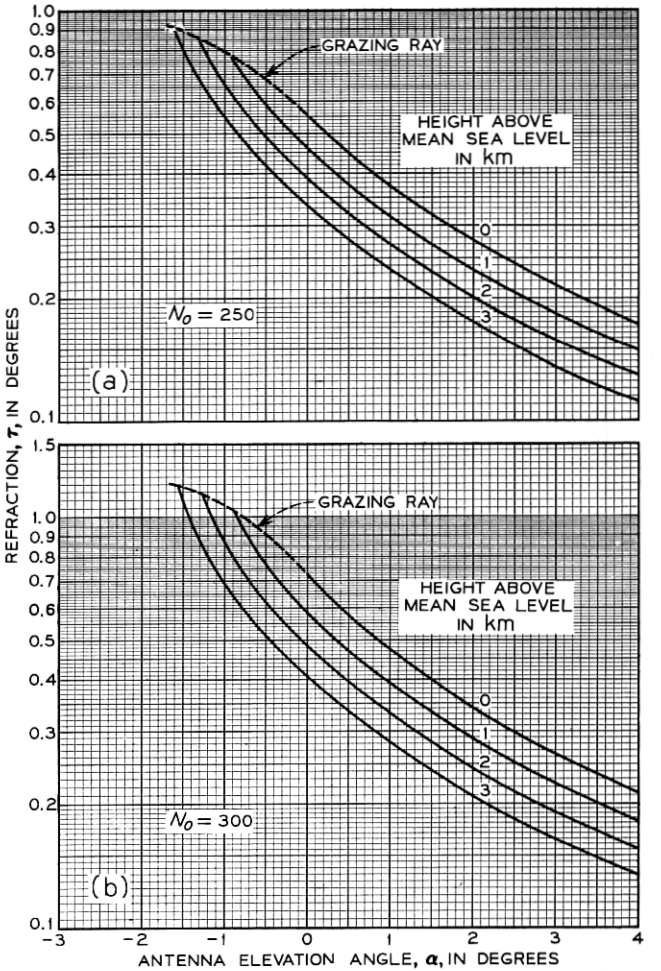

Fig. 6 — Refraction versus antenna elevation angle for (a) $N_o = 250$, and (b) $N_o = 300$.

other station heights, results in a family of curves (namely, h_s) for zero and positive initial ray angles.

2.2.2 *Negative Initial Angles* $(-\theta_o)$

The calculation of refraction for negative initial ray angles requires a modification of the technique used for positive angles. Note in Fig. 4 that the bending of the ray from T3$(h_3, -\theta_3)$ to T1 is the same as that

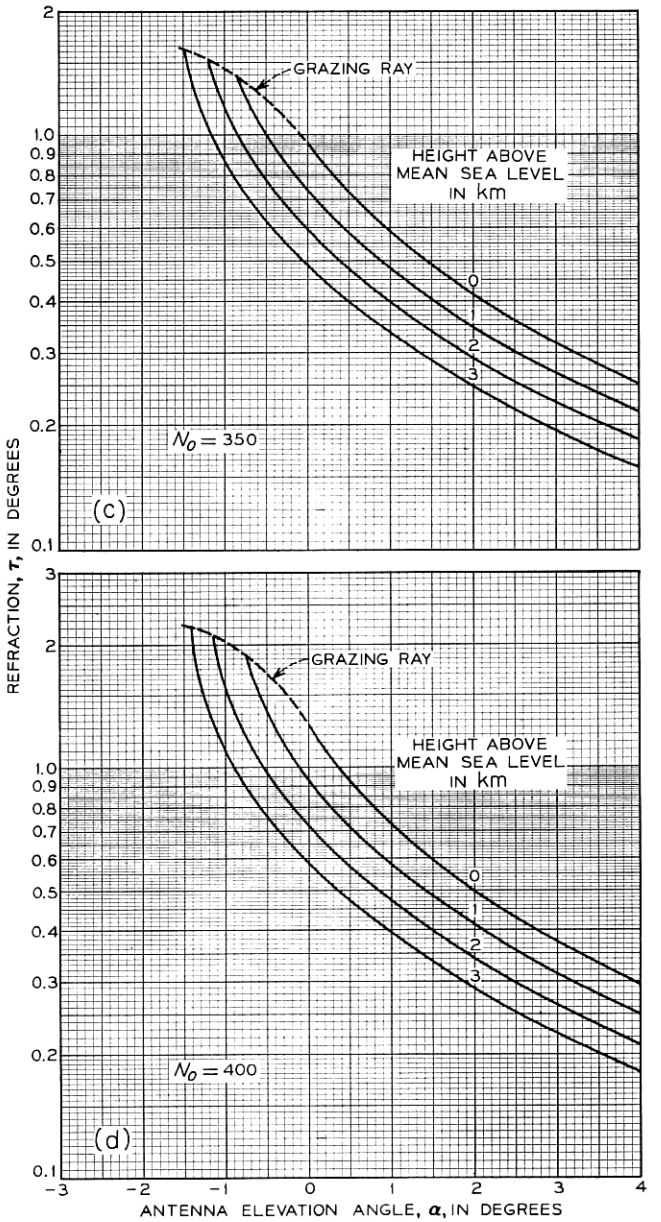

Fig. 6 — Refraction versus antenna elevation angle for (c) $N_o = 350$, and (d) $N_o = 400$.

of the ray from T1 (h_1 , $\theta_o = 0$) to T3. The latter is determined utilizing the equations for positive angles but in a slightly different manner.

First, assume a grazing ray ($h = 0$, $\theta_o = 0$) and, using the iterative method previously described, compute the bending τ and angle θ at each of the specific elevations h_s desired for the chart, that is, in the case of Figs. 6: 1, 2, and 3 km. The value of τ for each height is then added to the maximum τ determined for the same height (when θ_o is zero as found in Section 2.2.1) to obtain the total bending for a ray with the initial angle, $-\theta_o$. In Fig. 4 this is τ(T3, T1) plus τ(T1, S). Repeating the above but beginning with $h = 1$, 2, and so on, provides the data needed to extend the curves for positive initial angles into the negative range.

Note in Figs. 6 that all refraction curves terminate on a dotted extension of the zero-elevation ray representing a maximally refracted grazing ray. For a given height with an initial angle more negative than that represented by the point of termination, the ray is intercepted by the earth.

2.2.3 *Direct Machine Calculation*

For machine calculations it is desirable to compute the refractive bending directly without the use of refraction tables. For zero and positive initial ray angles, the calculation is straightforward as is described in Section 2.2.1. However, for a ray originating at a specific height with a negative initial angle θ_o , it is first necessary to determine the height of the ray where θ is zero (h_1 at T1 in Fig. 4). A variation of equation (5) permits this determination. If the right side of equation (5) represents point T1 in Fig. 4 and the left the initial station, say T3 at height h_3 , then

$$(1 + N_{T3} \times 10^{-6})(a + h_{T3}) \cos \theta_o = (1 + N_{T1} \times 10^{-6})(a + h_{T1}) = C. \quad (9)$$

The variables for the left side of equation (9) are all determined and evaluation yields the constant C. Then, values are assumed for h_{T1} beginning with zero, N_{T1} determined, and the right side evaluated until the result is equal to C. After h_{T1} is determined, τ(T3, T1) and τ(T1, S) are calculated as described in Section 2.2.2 and added numerically to give the total refractive bending. However, when h_{T1} is assumed to be 0 for the initial iteration and the right side is larger numerically than C, the beam intercepts the earth and a solution with angle θ_o is not possible. In such cases it is often desirable to determine the initial grazing-ray angle to the mean sea level horizon, which is accomplished by incrementing θ_o upward until the equation is satisfied.

2.2.4 *Angle from the Transmitting Site to the Radio Horizon*

The radio horizon, accounting for refraction and average local terrain, is determined by a variation of equation (9). Assuming that the height of a receiving station represents the average terrain height for some distance beyond, the initial angle α_H ($= \theta_o$) of a ray which just grazes the terrain represents the angle to the radio horizon as seen from an elevated transmitting site. Letting the left side of equation (9) represent the transmitting location, the right side the receiving location (where θ is zero), and solving for α_H yields

$$\alpha_H = \cos^{-1}\left[\frac{(1 + N_R \times 10^{-6})(a + h_R)}{(1 + N_T \times 10^{-6})(a + h_T)}\right] \text{ rad}, \qquad h_T \geqq h_R\ ,\ \alpha_H \leqq 0, \tag{10}$$

where the subscripts $_R$ and $_T$ refer to the receiving and transmitting stations, respectively. N_R is obtained by equation (4) and N_T by equations (1), (2), and (3), substituting N_R and h_R for N_s and h_s, and h_T for h. (For manual calculations, N_R and N_T may be determined from Figs. 5. First enter Fig. 5(a) with h_R , N_o , and read N_R from the ordinate. Then enter Fig. 5(b) with $(h_T - h_R)$, N_R and read N_T from the ordinate.)

2.2.5 *Refractive Index Limits*

We now illustrate the importance of including the effects of refraction in orbital computations relating to terrestrial radio-relay systems. Table I (reflecting the use of equations and techniques discussed in subsequent sections) demonstrates parametrically the sensitivity to radio refractivity of the orbit-intercept pointing azimuth and the computed terrestrial transmitter power limitation. The 8 dB variation in

TABLE I—INFLUENCE OF REFRACTION

Station Statistics	Assumed Values		
Path azimuth Station latitude Station elevation Antenna elevation angle α_o	103.5 degrees from true north 55.0° north mean sea level 0 degrees		
Parametric results	Computed values		
Radio refractivity N_s , N units	0	250	400
Geometric elevation angle, ϵ_o, degrees Critical azimuth (from north), degrees Maximum transmitter power, dBW	0 102.6 47	−0.555 101.76 50.7	−1.27 100.7 55

the power shown in the table indicates clearly that refraction must be included in calculations and that limits for refractivity should be carefully considered.

World charts of N_o in Ref. 8 indicate appropriate limits of N_o are 250 and 400. At specific locations and for short time intervals, the index may not fall within these limits. However, localized conditions will not affect large numbers of stations at any given time and a wider range of N_o would unnecessarily broaden the restrictive zone for radio-relay systems.

We suggest that the above limits be adopted for standardized calculations. For a specific case where an antenna pointing angle is close to the orbit and transmitter power limitations are restrictive, refractive limits applicable to that locale should be used.

2.2.6 *Adjustment of Computed Geometric Orbit Traces for Atmospheric Refraction*

For many solutions, particularly those involving graphical procedures, it is desirable to "elevate" a computed geometric orbit trace to its apparent (refracted) position and shape. Such an adjustment yields a presentation permitting a given, arbitrarily-shaped radio beam power profile to be related unrefracted and hence undistorted to the easily obtained configuration of the refracted orbit. Figures 7 are charts to enable this manipulation, produced from Figs. 6 by plotting $(\alpha - \tau_\alpha)$ versus τ_α. A method for using these charts is given in Section VI.

III. DETERMINATION OF THE POINTING AZIMUTH TO ORBIT INTERCEPT

Recall that the elevation angle (with respect to local horizontal) of the geometric director shown in Fig. 3 is denoted by ϵ. Hence, station geometric elevation angle ϵ_o may be replaced by $\alpha_o - \tau_{\alpha o}$ where α_o is the initial antenna beam elevation angle and $\tau_{\alpha o}$ is the corresponding refraction correction. (A method for determining α_o is given in Appendix A.)

Note that available information for established radio-relay routes in the United States giving antenna elevations, path distances, and antenna elevation angles is generally expressed in units of feet, statute miles, and degrees, respectively; it is necessary to convert these quantities into kilometers and radians for use in many of the expressions which follow.

Inspection of Fig. 8 shows that the azimuth displacement from the meridian through a station located at P to an intercept with the geo-

stationary orbit is identical to angle A of spherical triangle PES'. From laws for right spherical triangles

$$\cos A = \frac{\tan \varphi}{\tan \beta}, \tag{11}$$

where φ is the latitude at station P, and β is the arc equivalent of angle O of plane triangle OPS. Note that β is numerically equivalent to the maximum visible latitude for assumed radio-relay antenna beam elevation angle α_o and concomitant total ray-bending angle $\tau_{\alpha o}$.

Angle β is determined from triangle OPS using the Law of Sines. This triangle is redrawn in Fig. 9, where

$$\frac{\sin \Omega}{a} = \frac{\sin (\pi/2 + \epsilon_o)}{R},$$

$$\Omega = \sin^{-1} (K^{-1} \cos \epsilon_o), \tag{12}$$

where ϵ_o is the station geometric elevation angle corresponding to α_o, a is the earth radius, and R is the orbit radius, $R/a = K$. From inspection, $\beta = \pi/2 - \Omega - \epsilon_o$. Substituting for Ω yields

$$\beta = \cos^{-1} (K^{-1} \cos \epsilon_o) - \epsilon_o. \tag{13}$$

Substituting equation (13) for β in equation (11) results in

$$A = \cos^{-1} \left[\frac{\tan \varphi}{\tan [\cos^{-1} (K^{-1} \cos \epsilon_o) - \epsilon_o]} \right]. \tag{14}$$

IV. DETERMINATION OF RELATIVE LONGITUDE BETWEEN SITE AND ORBIT INTERCEPT

The earth longitude displacement between radio-relay site P and suborbital intercept S' in Fig. 8 is side λ of right spherical triangle PES'. From the Law of Sines

$$\frac{\sin \lambda}{\sin A} = \sin \beta,$$

from which:

$$\lambda = \sin^{-1} (\sin A \sin \beta), \tag{15}$$

where β and A are found by equations (13) and (14). Note that when $A = \pi/2$, corresponding to $\varphi = 0$, the maximum visible longitude displacement is β.

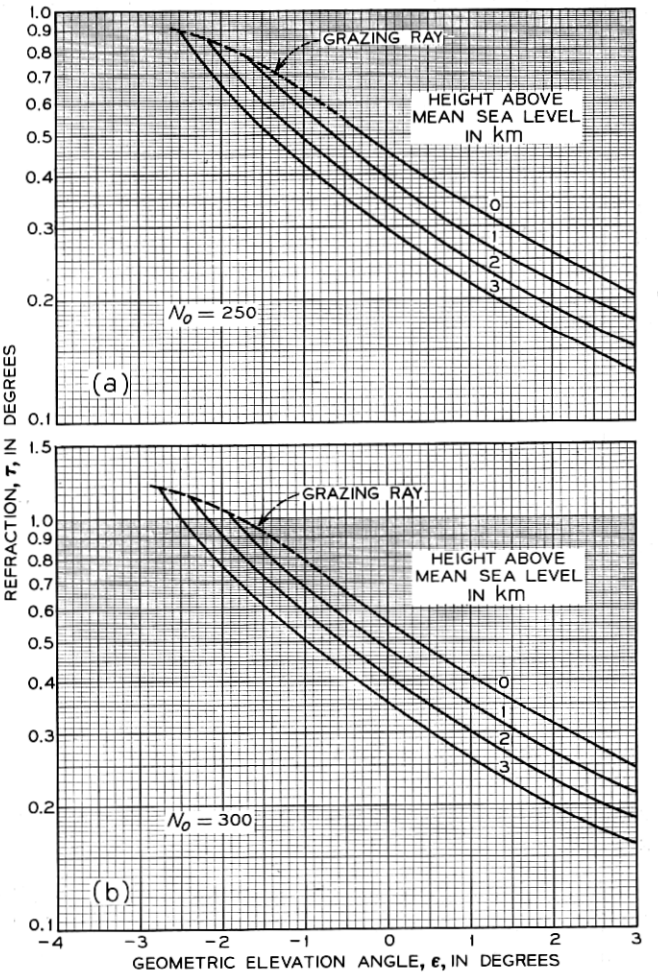

Fig. 7 — Refraction versus geometric elevation angle for (a) $N_0 = 250$, and (b) $N_0 = 300$.

V. GEOMETRIC ORBIT TRACE—CORRECTED FOR ANTENNA ELEVATION AND ATMOSPHERIC REFRACTION

The geostationary orbit and earth's equator are coplanar; hence the orbit near the horizon normally appears to be tilted with respect to the local horizontal plane. Were an equatorial orbit sufficiently distant, as in celestial observations, the angle of tilt would equal the colatitude

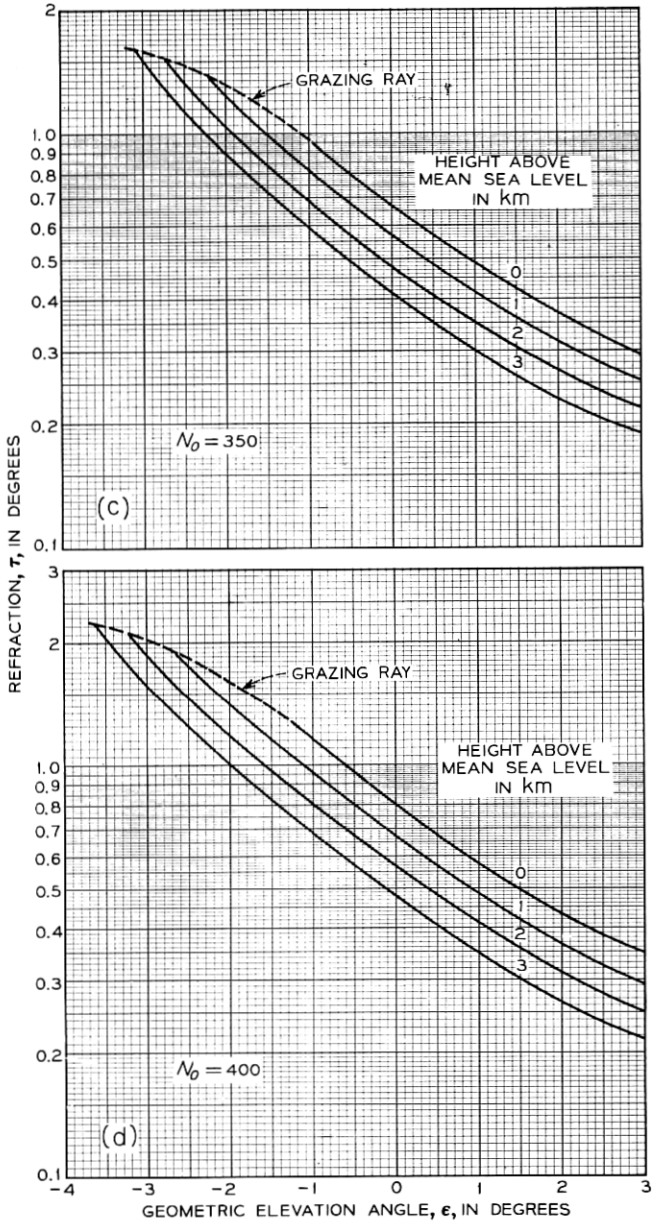

Fig. 7 — Refraction versus geometric elevation angle for (c) $N_0 = 350$, and (d) $N_0 = 400$.

of the observer's position. However, the maximum visibility circle in Fig. 8 is not a great circle, so the angle of tilt is less than the colatitude except where the latter circle crosses the equator. In the following paragraphs, an expression is developed for the tilt of the geostationary orbit as if viewed from a unique location on the visibility circle. This tilt is defined hereafter as the apparent slope of the orbit trace (or first deriva-

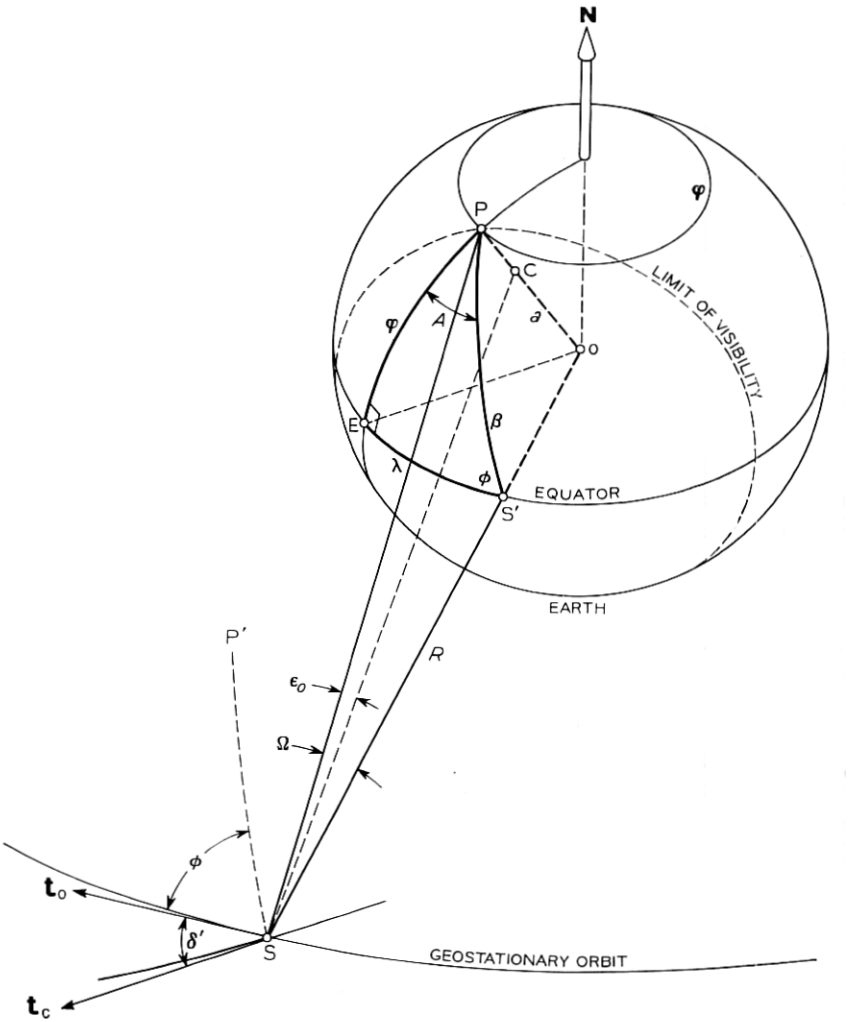

Fig. 8 — Geometry relating site P and geostationary orbit intercept.

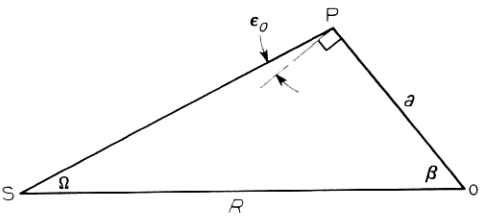

Fig. 9 — Geometry of intercept-determining triangle.

tive of the orbit trace, in elevation, with respect to direction, in azimuth).*

The size of the visibility circle in Fig. 8 depends upon α_o and $\tau_{\alpha o}$; for given site latitude φ, the angular displacement in earth longitude λ between site P and point S where the refracted beam intercepts the geostationary orbit (longitude of suborbital point S′) also depends upon α_o and $\tau_{\alpha o}$. Hence, the slope δ of the geometric orbit trace constructed in Fig. 11 also depends upon α_o and $\tau_{\alpha o}$.

Note in Fig. 8 that the angle between orbit tangent $\mathbf{t}_o$ constructed at S and the local vertical plane at P through S is angle ϕ of spherical triangle PES′. From the Law of Sines

$$\phi = \sin^{-1}\left(\frac{\sin\varphi}{\sin\beta}\right). \tag{16}$$

The complementary angle between orbit tangent $\mathbf{t}_o$ and the plane of a circle generated by radius CS (perpendicular to **OP**) is denoted by $\delta' = \pi/2 - \phi$. Substituting equation (16) for ϕ yields

$$\delta' = \cos^{-1}\left(\frac{\sin\varphi}{\sin\beta}\right). \tag{17}$$

Angle δ' is viewed in true magnitude from O (or S′), but is seen from radio-relay site P as a smaller angle δ when rotated through angle Ω as shown in Fig. 10. Note that $\tan\delta' = y/x$ and $\tan\delta = (y\cos\Omega)/x$, from which

$$\delta = \tan^{-1}(\tan\delta'\cos\Omega). \tag{18}$$

Combining equations (17) and (18) yields

$$\delta = \tan^{-1}\{\tan[\cos^{-1}(\sin\varphi/\sin\beta)]\cos\Omega\}. \tag{19}$$

* The orbit trace is envisioned as the locus of all pointing angles to the orbit, plotted on an azimuth-elevation chart aligned and calibrated according to the location of the observer.

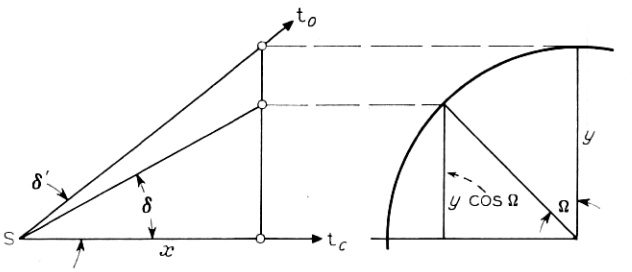

Fig. 10 — Development of geometric orbit slope as observed from site P.

VI. CONSTRUCTION OF THE REFRACTED ORBIT

Figure 11 presents the geometry of the problem viewed from a radio-relay station (similar, but not equivalent to the presentation given in Ref. 1). Reference to Figs. 1 and 3 may assist in interpretation of Fig. 11, wherein points A, S, and S_a correspond to similar points in Fig. 3 and intercept S corresponds to the left (easterly) intercept S in Fig. 1. Origin A is the beam-intercept direction from site P calculated from equation (14), accounting for atmospheric refraction.

Since the orbit is tilted with respect to the local horizontal plane at site P, the elevation angle of the geometric director to the orbit continuously varies as the orbit is scanned in azimuth. The refractive bending of a ray is a function of the geometric angle, so that the position of the apparent, or refracted orbit, is above the geometric orbit and it exhibits a constantly changing slope with respect to the latter.

The bent, refracted orbit is shown through point S_a (apparent position of interception point S with refraction; also, the antenna elevation angle α_o at the azimuth origin). The straight line labeled "geometric orbit" is tangent at S (Fig. 8) to a radial projection of the geostationary orbit on a sphere of radius PS centered at P. The horizontal line shown through S also represents an arc, in edge view of a great circle through S, parallel at S to the local horizontal plane at P, on this same sphere. Hence, the angle δ obtained from equation (19), corrected for refraction while retaining the concept of a constant site latitude φ, is also accurately represented by the apparent slope of the plane-figure geometric orbit trace at the azimuth origin. Figure 11 illustrates the construction of the corresponding refracted orbit trace.

The equation of the linear geometric orbit trace through S is

$$\epsilon' = -\tan(\delta)\triangle A + \alpha_o - \tau_{\alpha o}, \qquad (20)$$

where ϵ' is the elevation angle of the geometric orbit trace corresponding to an arbitrary displacement in azimuth $\triangle A$ from origin A.

Figs. 7 are entered with values of ϵ' derived from equation (20) to obtain total refractive ray-bending angles $\tau_{\epsilon'}$. The refracted orbit trace in Fig. 11 is then constructed by plotting points with coordinates $(A + \triangle A, \alpha')$ and connecting these with a smooth curve, where

$$\alpha' = \epsilon' + \tau_{\epsilon'} . \tag{21}$$

VII. Azimuth Displacement from Intercept to Keep the Beam Center an Angular Separation v from (and below) the Minimally Refracted Orbit (N_o minimum)

Figure 11 also illustrates a solution to keeping an angular separation v between the center of a circular beam and the geostationary orbit. The circle centered on S_a and labeled "unrefracted beam" is a cross-section of a conical figure of revolution with apex at antenna site P

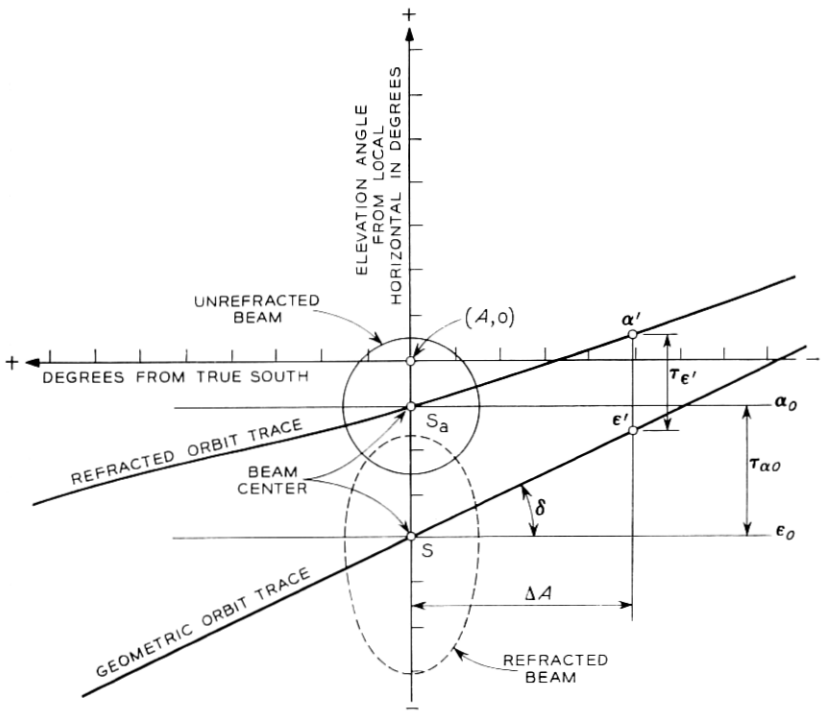

Fig. 11 — Orbit geometry as observed from site P.

and $2v$ included angle (locus of all rays having angle v with respect to the beam center). If elevation angle α_o of the antenna is fixed by radio-relay path parameters, the orbit can be avoided only by an azimuth displacement of the beam. The required angular separation v between the orbit and the beam center results when the latter is moved in azimuth away from intercept until the unrefracted cone is just tangent to the refracted orbit trace. Note that an identical relationship exists between the elongated "refracted beam" and the geometric orbit trace. However, since the former presentation is easier to develop and can readily accommodate unsymmetrical beam cross-sections, it is preferred for following analyses.

Figure 12 represents the analytical solution of an illustrative problem given in Appendix B and is helpful for visualizing subsequent procedures. From inspection

$$\tan \delta = \frac{(\alpha' - \tau_{\alpha'}) - (\alpha_o - \tau_{\alpha o})}{M}, \tag{22}$$

where α' is any point on the refracted orbit corresponding to arbitrary displacement M from an azimuth intercept. Note that in the range of interest M is negative with respect to azimuth $A_{\min}$, obtained from equation (14) using $\epsilon_o = \alpha_o - \tau_{\alpha o}$. Within a few degrees of intercept, the geometric orbit is approximated by a line of constant slope δ. Recall that adjustment of the geometric orbit for refraction results in a refracted orbit trace having a constantly changing slope with azimuth displacement from the intercept. This displacement for a given elevation of the refracted orbit is found by solving equation (22) for M:

$$M = \frac{(\alpha' - \tau_{\alpha'}) - (\alpha_o - \tau_{\alpha o})}{\tan \delta}. \tag{23}$$

Since the refracted orbit slope varies with elevation angle, no direct mathematical solution exists for determining that azimuth displacement providing an angular separation v between the beam center and the refracted orbit, measured in a direction normal to the latter. However, it is closely approximated by determining the slope of an orbit segment including the region of interest. Figure 12 suggests that the refracted orbit slope is everywhere less than the geometric slope. Hence, two judiciously chosen points on the refracted orbit having elevations

$$\alpha 1 = \alpha_o + v \cos \delta, \qquad \alpha 2 = \alpha_o + v,$$

always bracket the appropriate segment. Figures 6 and 12 also show that at these elevation angles the differential refraction is small. This

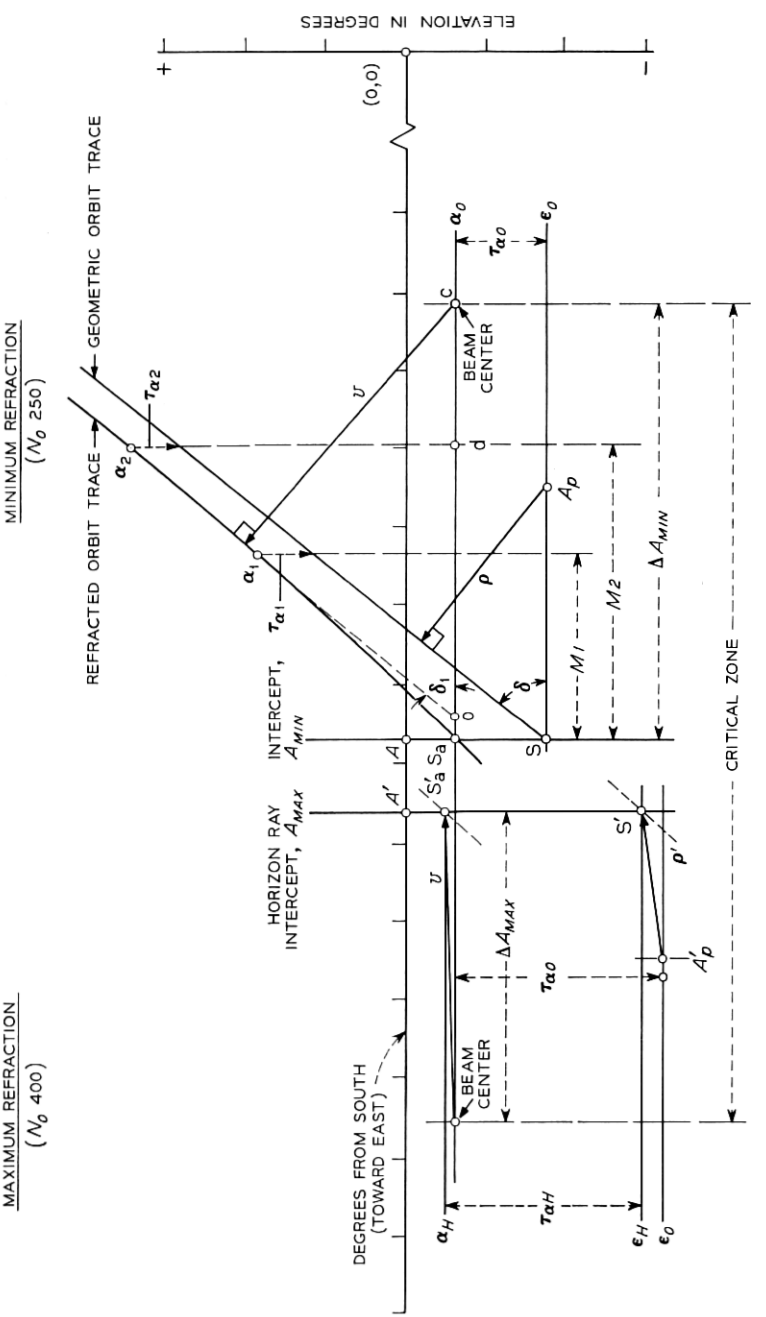

Fig. 12 — Graphical representation of the analytical solution.

supports the assumption that the slope of the small orbit segment in this region is virtually constant.

The refraction corresponding to elevation angles α_o, $\alpha 1$, and $\alpha 2$ are calculated or determined from the charts. Substituting α_o, $\tau_{\alpha o}$, $\alpha 1$, and $\tau_{\alpha 1}$ in equation (23) gives the azimuth displacement $M1$ corresponding to $\alpha 1$. Similarly, $M2$ is determined by substituting α_o, $\tau_{\alpha o}$, $\alpha 2$, and $\tau_{\alpha 2}$. Slope $\delta 1$ between the two chosen points on the refracted orbit is given by

$$\tan \delta 1 = (\alpha 2 - \alpha 1)/(M2 - M1),$$

resulting in

$$\delta 1 = \tan^{-1} [v(1 - \cos \delta)/\triangle M], \tag{24}$$

where $\triangle M = M2 - M1$.

Figure 12 shows that azimuth displacement $\triangle A$ necessary to keep the beam center an angular separation v from the refracted orbit is $S_a c$ (equal to $S_a o$ plus oc).* By inspection, $oc = v/\sin \delta 1$, $od = v/\tan \delta 1$ and $S_a o = M2 - od$. Assembling these into an equation for $\triangle A$ yields

$$\triangle A_{\min} = M2 - v/\tan \delta 1 + v/\sin \delta 1. \tag{25}$$

7.1 *Special Case*

If a ray with initial angle α_o intercepts the earth, a solution is obtained by calculating angle α_H to the radio horizon as is described in Section II. Then, substituting ϵ_H for ϵ_o in equation (14), the orbit intercept for a grazing ray is determined. When solving for the necessary azimuth displacement from this intercept, α_H and $\tau_{\alpha H}$ are substituted for α_o and $\tau_{\alpha o}$ in equation (23). Note, however, that in determining $\alpha 1$ and $\alpha 2$ for substitution in equation (23), the use of ray angle α_o remains valid.

VIII. Azimuth Displacement from Intercept to Keep the Beam Center an Angular Separation v from (and above) the Maximally Refracted Orbit (N_o maximum)

The left side of Fig. 12 shows that the refracted orbit for the case of maximum refraction falls below the radio horizon with azimuth displacement from point $A_{\max}$ obtained from equation (14) using $\epsilon_H = \alpha_H - \tau_{\alpha H}$. Since the earth intercepts all rays below the horizon, they cannot affect the orbit and it is only necessary to displace the beam

* Notations such as $S_a c$ represent scalar distances between indicated points in Fig. 12.

center in azimuth sufficiently to maintain angular separation v from the horizon intercept. The required displacement is

$$\triangle A_{\max} = [v^2 - (\alpha_o - \alpha_H)^2]^{\frac{1}{2}}. \quad (26)$$

In Fig. 12, $\alpha_H(-0.25°)$ is the initial angle of a ray which grazes at a receiving station height of 0.4 km and originates at an assumed transmitting height of 0.5 km.

As demonstrated in Appendix B, little increase in the critical zone results if it is assumed that the angle to the radio horizon is equal to the initial ray angle. Therefore, for manual calculations involving small positive values of α_o, these angles are assumed identical so that $\triangle A$ is simply an angular separation v from the orbit intercept determined for α_o. For values of α_o more negative than that for a grazing ray (determined from Figs. 6 or by calculation), it is necessary to determine α_H and the corresponding orbit intercept using equations (10) and (14). Then equation (26) gives the necessary azimuth displacement.

IX. DETERMINATION OF THE CRITICAL ZONES

9.1 *Critical Zones Defined*

The critical zones to be avoided at radio-relay transmitting sites to protect the geostationary orbit are defined:

$$Z_{crit} = A_{\max} + \triangle A_{\max} \quad \text{to} \quad A_{\min} - \triangle A_{\min}$$

(degrees from South), (27)

where values for A and $\triangle A$ for maximum and minimum refraction are obtained as in Sections III, VII, and VIII. These zones are converted to azimuth zones with respect to true north by subtracting the boundaries from 180 degrees for the easterly zone and adding them to 180 degrees for the westerly zone.

Calculations for stations in southern latitudes are identical except that they are referenced to north rather than south. The easterly azimuth zone with respect to true north is obtained directly from equation (27), while the zone boundaries are subtracted from 360 degrees for the westerly zone.

9.2 *Special Case*

At latitudes exceeding $\varphi = \cos^{-1}(K^{-1}\cos\Psi) - \Psi$ it is impossible for the beam's center ray to be below the orbit with angular separation v.* Hence, for such extreme northern latitudes, a single critical zone

* Derivation of this equation is given in Appendix C.

spans south with both easterly and westerly boundaries defined by

$$Z_{crit} = A_{max} + \triangle A_{max} \quad \text{(degrees from south)}. \tag{28}$$

X. DETERMINATION OF MAXIMUM PERMISSIBLE RADIATED POWER

As mentioned in Section I, international agreements exist for maximum radiated powers.[9] For 6-GHz radio-relay transmitters whose antennas point within $v = 2°$ of the geostationary orbit, the power limitation for separations less than 0.5° is 47 dBW relative to the isotropic case (EIRP), increasing 8 dB per degree to a maximum of 55 dBW (occurring at 1.5°). This limitation refers specifically to the center of the major lobe. For this case, only the relationship between the refracted center ray of the beam and the geometric orbit is considered.

If an existing or proposed path direction is between the critical values computed as in Section III for maximum and minimum refraction, the refracted center ray is likely to intercept the orbit for appreciable periods of time. For such cases the maximum power is 47 dBW.

If the path direction for a system in the northern hemisphere is within the critical zone but nearer to south (smaller) than A_{min}, the actual separation ρ illustrated in Fig. 12 is

$$\rho = (A_{min} - A_p) \sin \delta, \tag{29}$$

where A_p is the path direction measured from true south.

Conversely, if A_p exceeds A_{max}, the separation of the beam center from intercept of the geometric orbit and the refracted horizon (Fig. 12) is

$$\rho = [(A_p - A_{max})^2 + | \epsilon_H - \epsilon_o |^2]^{\frac{1}{2}}, \tag{30}$$

where

$$\epsilon_H = \alpha_H - \tau_{\alpha H}, \qquad \epsilon_o = \alpha_o - \tau_{\alpha o}.$$

Note that ϵ_o in equation (30) represents maximum atmospheric refraction.

If a ray having initial angle α_o intercepts the earth, ϵ_o for use in equation (30) is indeterminate. For such special cases, a conservative approximation for the angular separation is $\rho = A_p - A_{max}$.

The maximum permissible effective radiated power P_t dBW (EIRP) is given for separation ρ according to the following criteria:

$$\rho \leqq 0.5°, \qquad P_t = 47;$$

$$0.5° < \rho \leqq 1.5°, \quad P_t = 8(\rho - 0.5) + 47; \tag{31}$$
$$\rho > 1.5°, \quad P_t = 55.$$

XI. CONCLUSIONS

A direct analytical method involving few approximations and assumptions can be used by system planners for calculating refraction-corrected ranges of pointing azimuth for microwave radio-relay antennas within which significant interference with geostationary communication satellites can be expected. Required angular separations between the refracted beam and the geostationary orbit are translated into required azimuth displacements of a radio-relay antenna from that calculated for orbit intercept; conversely, for cases where exposure is unavoidable, means for determining the maximum transmitted powers permitted by international agreement are presented.

Since all analytical expressions including refraction corrections are readily amenable to machine calculation, both speed and improved accuracy in estimating the pointing azimuths are possible. The suggested refractive index limits are believed to be representative for the large majority of exposures and useful for a standardized approach to the problem. For more general applications, where refractive index variations are known to be different, one may use the same principles to generate his own applicable correction curves.

XII. ACKNOWLEDGMENTS

The authors wish to express appreciation to R. C. Harris for motivating this presentation, to G. D. Thayer of the U. S. Department of Commerce, Environmental Science Services Administration, for encouragement in the treatment of refraction for negative angles, and to J. L. Boyette for assistance in mathematical programming.

APPENDIX A

Estimation of Antenna Elevation Angles

The initial beam elevation angle for a radio-relay antenna is determined by the geometry of transmitting and receiving locations, the path length, and refraction. The final alignment based upon transmission measurements, if recorded, is preferred for these calculations. The antenna elevation angle for proposed radio-relay paths can be estimated using the method given below with sufficient accuracy.

Figure 13 depicts radio-relay transmitter T and receiver R at elevations OT and OR above geocenter O, assuming a spherical earth of radius ka. Coefficient k is the ratio of apparent earth radius to true earth radius and accounts for refraction in the lower atmosphere.[10] The path length is represented by arc $\hat{D}$ (great circle length at mean sea level). The transmitting and receiving antenna heights with respect to mean sea level are denoted by h_T and h_R, respectively.

Inspecting Fig. 13, $\phi = \hat{D}/ka$ radians, $C' = 2(ka + h_T) \sin(\phi/2)$, and $\alpha_o = E - \phi/2$ radians. From triangle TT'R and laws for plane triangles

$$\tan E = \frac{(h_R - h_T) \sin(\pi/2 - \phi/2)}{C' + (h_R - h_T) \cos(\pi/2 - \phi/2)}. \tag{32}$$

It can also be shown that

$$\alpha_o = \tan^{-1}\left[\frac{h_R - h_T}{\tan(\hat{D}/2ka) \times (2ka + h_R + h_T)}\right] - \hat{D}/2ka \text{ radians}, \tag{33}$$

where h_R, h_T, $\hat{D}$, and a are expressed in the same units.

Reference 2 provides a formula and a table relating k and N_s. For most calculations, a value of $k = \frac{4}{3}$ results in sufficient accuracy[10] (the

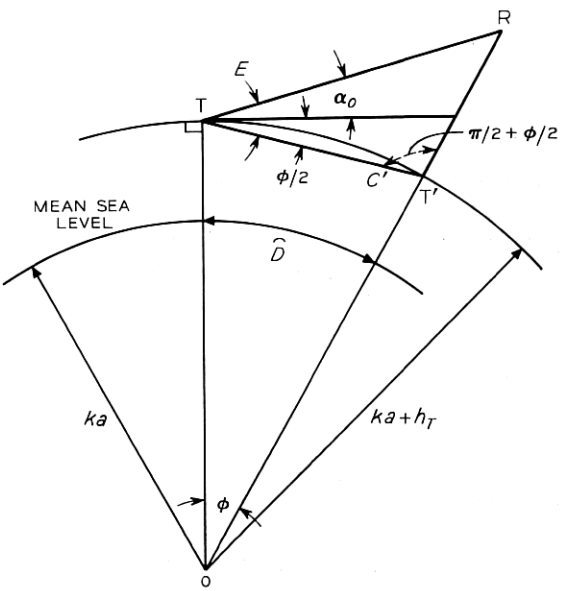

Fig. 13 — Geometry of antenna elevation angle.

geometries of radio-relay systems within limits of normal site elevations require antenna elevation angles which are relatively insensitive to values chosen for k).

APPENDIX B

Illustrative Calculation

Problem Input for a Particular Radio-Relay Site:

Latitude φ	— 38°N,
Transmitter Height h_T	— 0.5 km,
Receiver Height h_R	— 0.4 km,
Path Length $\hat{D}$	— 28 km,
Path Azimuth A_p	— 97.75° with respect to true north, equivalent to 82.25° from south towards east,
N_o Limits	— 250 and 400 N units.

B.1 *Antenna Elevation Angle*

From equation (33) and using $k = \frac{4}{3}$

$$\alpha_o = \tan^{-1}\left[\frac{0.4 - 0.5}{\tan\left[(28/(2.66 \times 6373)\right](2.66 \times 6373 + 0.4 + 0.5)}\right] - \frac{28}{2.66 \times 6373}$$

$$= -0.00523 \text{ rad, which converts to } -0.3°.$$

B.2 *Geometric Elevation Angle for $N_o = 250$*

From Fig. 6a

$$\epsilon_o = \alpha_o - \tau_{\alpha o} = -0.3 - 0.59 = -0.89°.$$

B.3 *Azimuth Intercept for $N_o = 250$*

From equations (13) and (14)

$$\beta = \cos^{-1}\left[0.1509 \cos (0.89°)\right] + 0.89 = 82.2°,$$

$$A_{\min} = \cos^{-1}\left[\tan (38°)/\tan (82.2°)\right] = 83.86° \text{ from south.}$$

B.4 *Orbit Slope for $N_o = 250$*

From equations (12) and (19)

$$\Omega = \sin^{-1}\left[0.1509 \cos (0.89°)\right] = 8.68°,$$

$$\delta = \tan^{-1}\left[\tan\left\{\cos^{-1}\left[\sin (38°)/\sin (82.2°)\right]\right\} \cos (8.68°)\right] = 51.26°.$$

B.5 *Azimuth Displacement for $v = 2°$ below the Orbit*

From equations (23), (24), (25), and Fig. 6(a)

$$\alpha_o = -0.3°, \qquad \tau_{\alpha o} = 0.59°,$$

$$\alpha 1 = -0.3 + 2\cos(51.26°) = 0.95°, \qquad \tau_{\alpha 1} = 0.35°,$$

$$\alpha 2 = -0.3 + 2 = 1.7°, \qquad \tau_{\alpha 2} = 0.28°,$$

$$M1 = [(0.95 - 0.35) - (-0.3 - 0.59)] \div \tan(51.26°) = 1.19°,$$

$$M2 = [(1.7 - 0.28) - (-0.3 - 0.59)] \div \tan(51.26°) = 1.85°,$$

$$\delta 1 = \tan^{-1}\{2[1 - \cos(51.26°)]/0.66\} = 48.62°,$$

$$\triangle A_{\min} = 1.85 - 2/\tan(48.62°) + 2/\sin(48.62°)$$

$$= 2.76° \text{ toward south from intercept.}$$

B.6 *Horizon Intercept for $N_o = 400$*

From equations (1), (2), (3), (4), (10), (12), (13), (14), and Fig. 6(d)

$$N_R = 400 \exp(-0.4/7) = 377.78 \text{ or from Fig. 5(a)},$$

$$\triangle N = -7.32 \exp(0.005577 \times 377.78) = -60.2,$$

$$C_e = \ln[377.78/(377.78 - 60.2)] = 0.17,$$

$$N_T = 377.78 \exp[-0.17(0.5 - 0.4)] = 371.28 \text{ or from Fig. 5(b)},$$

$$\alpha_H = -\cos^{-1}\left[\frac{1.000377}{1.000371} \times \frac{6373.4}{6373.5}\right] = -0.25°,$$

$$\tau_{\alpha H} = 1.22°,$$

$$\epsilon_H = -0.25 - 1.22 = -1.47°,$$

$$\beta = \cos^{-1}[0.1509\cos(1.47°)] + 1.47 = 82.79°,$$

$$A_{\max} = \cos^{-1}[\tan(38°)/\tan(82.79°)] = 84.33° \text{ from south.}$$

B.7 *Azimuth Displacement for $v = 2°$ from Horizon Intercept*

From equation (26)

$$\triangle A_{\max} = [(2)^2 - (-0.3 + 0.25)^2]^{\frac{1}{2}}$$

$$= 1.99° \text{ toward north from intercept.}$$

B.8 *Critical Zone*

From equation (27)

$$Z_{crit} = 84.33 + 1.99 \quad \text{to} \quad 83.86 - 2.76$$
$$= 86.3° \quad \text{to} \quad 81.1° \text{ from south.}$$

B.9 *Azimuthal Zones*

True-north azimuths:

93.7° to 98.9° easterly, and

266.3° to 261.1° westerly.

The path azimuth of 97.75° falls within the easterly azimuthal zone.

B.10 *Relative Longitude to Suborbit Intercepts*

From equation (15)

$$\lambda_{min} = \sin^{-1} [\sin (83.86°) \sin (82.2°)] = 80.04°,$$

$$\lambda_{max} = \sin^{-1} [\sin (84.33°) \sin (82.79°)] = 80.82°.$$

B.11 *Maximum Permissible Radiated Power*

Comparing the path direction of 82.25° from south with the critical zone found in Section B.8 and with A_{min} and A_{max} found in Sections B.3 and B.6 reveals that equations (29) and (31) are appropriate for calculating the angular separation and permissible power:

$$\rho = (83.86 - 82.25) \sin (51.26°) = 1.23°,$$

$$P_t = 8(1.23 - 0.5) + 47 = 52.8 \text{ dBW} \quad \text{at} \quad 6 \text{ GHz}.$$

B.11.1 *Alternate Power Calculation*

An alternate calculation is indicated when the path direction is further from south than A_{max}. Assume that A_p is, instead, 85.25° from south (left side of Fig. 12). The appropriate equations are now (30) and (31). A value of ϵ_o for maximum refraction is required for equation (30). From Section B.5, Fig. 6(d), equations (30) and (31)

$$\alpha_o = -0.3°,$$

$$\tau_{ao} = 1.3°,$$

$$\epsilon_o = -1.6°,$$

$$\rho = [(85.25 - 84.33)^2 + (-1.47 + 1.6)^2]^{\frac{1}{2}} = 0.93°,$$

$$P_t = 8(0.93 - 0.5) + 47 = 50.4 \text{ dBW at 6 GHz}.$$

APPENDIX C

Alternate Derivations of Basic Equations and Critical Latitudes

All following relationships are expressed in terms of latitude φ of radio-relay site P_v shown in Fig. 14 (a constant), and the maximum latitude for which the refracted geostationary orbit is visible to the antenna (a constant elevation angle).

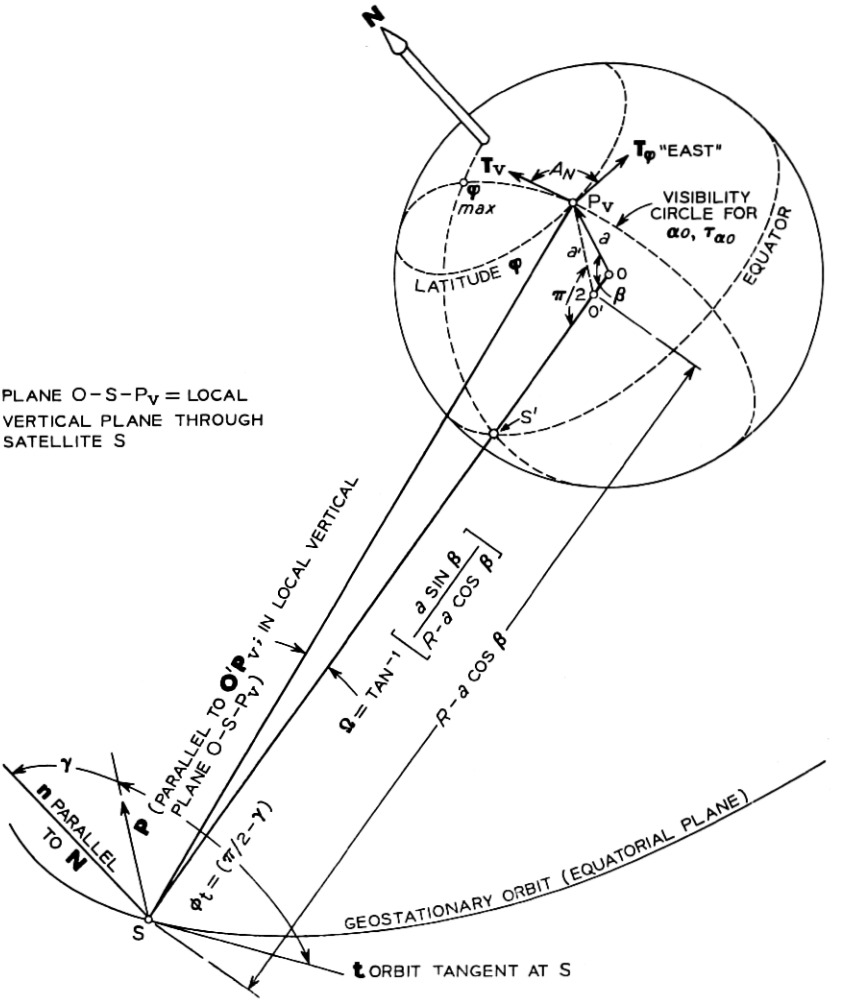

Fig. 14 — Angle ϕ_t between orbit tangent and local vertical plane O-S-P_v.

C.1 *Latitude Limit of Visibility for the Geostationary Orbit*

Figure 14 shows that the maximum latitude visible to the geostationary orbit is

$$\begin{aligned} \varphi_{\max} &= \cos^{-1}\left[K^{-1}\cos\left(\alpha_o - \tau_{\alpha o}\right)\right] - \alpha_o - \tau_{\alpha o} \\ &= \beta, \end{aligned} \tag{34}$$

where

α_o = known elevation angle of the radio-relay antenna,
$\tau_{\alpha o}$ = corresponding total ray-bending angle due to refraction inferred from CRPL Exponential Reference Atmosphere[2] or from Figs. 6 of text, and
K = ratio of orbit radius R to assumed earth radius a.

Hence, equation (34) is a restatement of equation (13).

C.2 *Pointing Azimuth to Orbit Intercept*

The larger of angles formed by intersection of site latitude circle φ and the visibility circle corrected for antenna elevation and refraction shown in Fig. 14 is a direct measure of the pointing azimuth to be avoided for a station located at that intersection (P_v). Hence, angle A_N between tangents $\mathbf{T}_\varphi$ and $\mathbf{T}_v$ is the supplement of pointing angle A given by equation (14) referred to true south. From the geometry of Fig. 14

$$\begin{aligned} A_N = \cos^{-1}\Bigg\{ &-\sin\left[\tan^{-1}\left(\frac{\sin\varphi}{|\,(1-\sin^2\varphi-\cos^2\beta)^{\frac{1}{2}}\,|}\right)\right] \\ &\cdot\cos\left[\tan^{-1}\left(\frac{|\,(1-\sin^2\varphi-\cos^2\beta)^{\frac{1}{2}}\,|}{\cos\beta}\right)\right]\Bigg\}, \end{aligned}$$

$$\pi/2 \leqq |\,A_N\,| < \pi. \tag{35}$$

Equation (35) yields two pointing azimuths which are of interest; one in the second quadrant referred to true north, corresponding to a westerly direction for stations in the northern hemisphere—and one in the third quadrant, or easterly direction. Reversed directions result for stations in the southern latitudes.

Figures 15 illustrate changes of variables which simplify the demonstration of equivalence between equation (35) and equation (14). Since $\cos^2\beta = 1 - \sin^2\beta$ and $\cos^2\varphi = 1 - \sin^2\varphi$,

$$A_N = \cos^{-1}\left\{-\sin\left[\tan^{-1}\left(\frac{\sin\varphi}{|\,(\sin^2\beta-\sin^2\varphi)^{\frac{1}{2}}\,|}\right)\right]\right.$$

$$\cdot \cos\left[\tan^{-1}\left(\frac{|\,(\cos^2\varphi - \cos^2\beta)^{\frac{1}{2}}\,|}{\cos\beta}\right)\right]\Bigg\}.$$

Substituting μ and ν (Figs. 15) and reducing the result yields

$$A_N = \cos^{-1}(-\sin\mu\cos\nu).$$

Now, substituting for μ and ν provides

$$\begin{aligned} A_N &= \cos^{-1}[-(\sin\varphi/\sin\beta)(\cos\beta/\cos\varphi)] \\ &= \cos^{-1}\left(-\frac{\tan\varphi}{\tan\beta}\right), \end{aligned}$$

which is exactly the supplement of the angle obtained from equation (11) in the text.

C.3 *Longitude Displacement of Orbit Intercept*

The earth-longitude displacement between radio-relay site P_v and suborbital intercept S′ in Fig. 14 is also inferred from equation (35):

$$\begin{aligned} \lambda &= \tan^{-1}\left[\frac{|\,(1 - \sin^2\varphi - \cos^2\beta)^{\frac{1}{2}}\,|}{\cos\beta}\right] \qquad 0 \leqq |\,\lambda\,| < \pi/2, \\ &= \sin^{-1}(\sin A \sin\beta), \end{aligned} \tag{36}$$

from which first and fourth quadrant longitude adjustments are referred to the suborbital longitude. The equivalence with equation (15) is demonstrated using techniques indicated above and identifying angle β uniquely with the maximum latitude for visibility φ_{max} (Section C.1).

C.4 *Geometric Orbit Trace*

Since the size of the visibility circle in Fig. 14 depends upon α_o and $\tau_{\alpha o}$, the earth-longitude displacement λ between P_v and S (same longitude as suborbital point S′) also depends upon α_o and $\tau_{\alpha o}$. Because

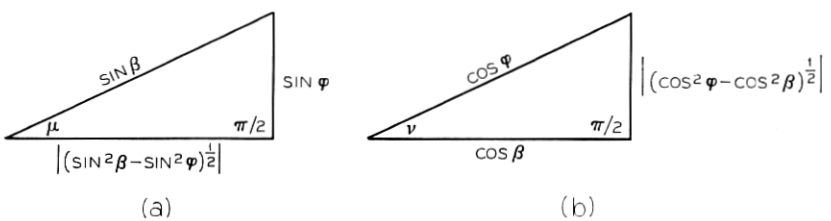

Fig. 15 — Change of variables: (a) angle μ and (b) angle ν.

the resulting viewing aspect depends upon these parameters, the slope of the geometrical orbit trace constructed in Fig. 11 also depends upon α_o and $\tau_{\alpha o}$ as well as φ.

Note that the angle between orbit tangent **t** constructed at S and the local vertical plane at P_v through S is denoted by ϕ_t. This angle is observed undistorted at point S′, but appears to be a slightly enlarged angle ϕ_t' for an observer at P_v (as if point S were visible without ray bending):

$$\phi_t' = \tan^{-1} (\tan \phi_t / \cos \Omega). \tag{37}$$

Hence, complementary angle δ between orbit tangent **t** and a line through S perpendicular to the geometrical line-of-sight $\mathbf{SP}_v$ and parallel to the horizontal plane at P_v is also the slope of the corrected geometric orbit trace shown in Fig. 11,

$$\begin{aligned} \delta &= \cot^{-1} (\tan \phi_t / \cos \Omega) \\ &= \cot^{-1} \left\{ \frac{\tan [\sin^{-1} (\sin \varphi / \sin \beta)]}{\cos \{\tan^{-1} [\sin \beta / (K - \cos \beta)]\}} \right\} \\ &= \tan^{-1} \{\tan [\cos^{-1} (\sin \varphi / \sin \beta)] \cos \Omega\}, \end{aligned} \tag{38}$$

for which equivalence to equation (19) is shown using the techniques incorporated in Sections C.2 and C.3.

C.5 *Maximum Latitude Permitting Angular Separation v Below the Orbit*

A maximum latitude exists for each antenna elevation angle allowing the beam-center ray to be below the refracted orbit with prescribed angular separation v. Figure 16 illustrates the determination of this critical latitude. S_p is a point on the geostationary orbit having zero relative longitude with respect to station site P_v. A ray emanating from the antenna with initial vertical angle $(\pi/2 + \alpha_o + v)$ must just intercept the orbit. Accounting for refraction, the angle between the geo-

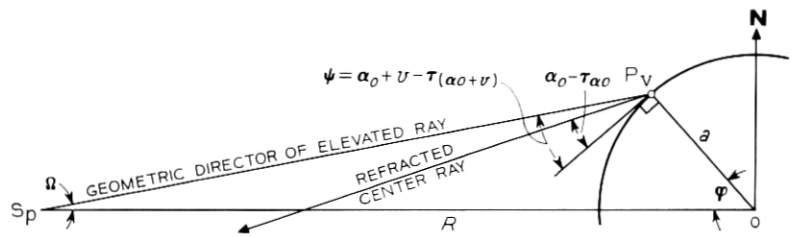

Fig. 16 — Geometry determining the critical latitude.

metric director of the elevated ray and the local horizontal is $\Psi = [\alpha_o + v - \tau_{(\alpha_o+v)}]$. Site latitude φ and Ψ are related by triangle OP_vS_p. From the Law of Sines

$$\frac{\sin(\pi/2 + \Psi)}{R} = \frac{\sin \Omega}{a}.$$

Letting $R/a = K$,

$$\Omega = \sin^{-1}(K^{-1} \cos \Psi).$$

Since $\Omega + \varphi + \pi/2 + \Psi = \pi$,

$$\varphi = \cos^{-1}(K^{-1} \cos \Psi) - \Psi. \tag{39}$$

REFERENCES

1. Gould, R. G., "Protection of the Stationary Satellite Orbit," Telecommunication J., *34*, No. 8 (August 1967), pp. 307–312.
2. Bean, B. R., and Thayer, G. D., "CRPL Exponential Reference Atmosphere," NBS Monograph 4, U. S. Department of Commerce, Washington, D. C., October 29, 1959.
3. Brice, P. J., "Total Atmospheric Refraction of Radio Waves at Small Angles of Declination," unpublished work (WO Branch Memorandum p. 326), Post Office Research Station, General Post Office, London, February, 1967.
4. Lundgren, C. W., unpublished work.
5. Bean, B. R., and Dutton, E. J., "Radio Meteorology," NBS Monograph 92, U. S. Department of Commerce, Washington, D. C., March 1, 1966, p. 345.
6. Bean, B R., "The Radio Refractive Index of Air," Proc. IRE, *50*, No. 3 (March 1962), pp. 260–273.
7. Schulkin, M., "Average Radio-Ray Refraction in the Lower Atmosphere," Proc. IRE, *40*, No. 5 (May 1952), pp. 554–561.
8. Bean, B. R., Horn, J. D., and Ozanich, Jr., A. M. "Climatic Charts and Data of the Radio Refractive Index for the United States and the World," NBS Monograph 22, U S. Department of Commerce, Washington, D. C., November 25, 1960.
9. CCIR Recommendation 406-1, *Documents of the XI Plenary Assembly, Oslo*, 1966, *4*, Part 1.
10. Schelleng, J. C., Burrows, C. R., and Ferrell, E. G., "Ultra-Short-Wave Propagation," Proc. IRE, *21*, No. 3 (March 1933), pp. 427–463.